Construction and Building Materials 346 (2022) 128392

Contents lists available at ScienceDirect

Construction and Building Materials

journal homepage: www.elsevier.com/locate/conbuildmat

Low-energy lightweight aggregates by cold bonding of biomass wastes: Effects of raw material proportion adjustments on product properties

Ricardo Serpell *, Daia Zwicky

Institut de Technologies de l'Environnement Construit, iTEC, Haute école d'ingénierie et d'architecture de Fribourg, HEIA-FR, HES-SO University of Applied Sciences and Arts Western Switzerland

ARTICLE INFO

Keywords:
Cold-bonding
Lightweight aggregates
Biomass wastes
Low-energy construction materials
Pelletizing

ABSTRACT

The reported research explored the feasibility of cold bonding as a method to produce low-embodied-energy lightweight aggregates from locally available biomass wastes (wood sawdust and ashes) and cement, using response surface methodology to model the effect of raw material proportions on the properties of the product. The empirical exploration comprised the particle size distribution, saturated surface dry and oven dry density, water absorption capacity, drying shrinkage, short- (7 days) and long-term (70-days) particle crushing strength, and strength variability of the pellets. Aggregates with particle densities below 1.850 g/cm^3 and crushing strengths above 1.5 MPa (comparable to expanded clay aggregates) were obtained. In the experimental region explored, increasing sawdust contents to decrease aggregate density negatively affected all the other aggregate properties tested. However, the negative impact was strongly reduced by increasing the ratio of coarse particles in the sawdust. Intermixing cement in the raw material mixture – as opposed to adding it as a coating to the already formed pellets – resulted in better formed, smaller, and stronger pellets, and reduced strength variability. The response model obtained was validated and used to optimize aggregate properties with the specific set of raw materials and production methods studied.

1. Introduction

Concrete fulfills structural and non-structural roles in almost every building type, including lightweight construction. As showcased in the construction details of recent mid-rise timber buildings (e.g. [1]), in addition to as a material for underground structures, timber-based lightweight construction makes ample use of concrete in above-ground parts of the building, e.g. to provide acoustic insulation, thermal mass, fire protection or additional structural stiffness. Materials for these applications are usually selected from readily available structural concrete. In doing so, relevant aspects of the material's contribution to overall building performance escape the control of designers. Functional requirements are met with sub-optimal use of resources: structural concretes are overly strong and heavy, increasing required dimensions of other structural elements and, in this way, adding unnecessarily to the environmental footprint of timber buildings. Although lightweight aggregates (LWA) can be used to formulate lighter concretes, LWA are energy intensive and correspondingly expensive, which limits their environmental contribution and hinder their widespread use in timber construction. Whereas conventional aggregates add around 5 kgCO_2eq to the global warming potential of concrete (on average 230 kgCO_2eq/m^3 [2]), LWA can add up to 150 kgCO_2eq to it [3]. As a consequence, potential environmental benefits accruing from reductions in material quantities (e.g. smaller structural cross-sections) made possible by the use of lightweight concrete can be outweighed by the LWA's own embodied energy and global warming potential.

Organic-based lightweight concretes have been proposed as a timber-compatible alternative [4–8]. Wood-cement composites (WCC) can be produced by bonding lignocellulosic materials (such as wood sawdust) with Portland cement or other inorganic binders [8,9]. Compared to wood-resin composites, WCC exhibit higher durability, dimensional stability, fire and biodegradation resistance, while weighing less than half as much as a sand-cement mortar [10]. These properties make them suitable for interior and exterior applications in construction, where they are used mostly in prefabricated panels. The production of WCC also provides a viable alternative to recycle wood wastes, not only from the timber industry but also from construction and demolition [11]. The main concern when dealing with different wood sources is their potential incompatibilities with cement (e.g. impaired cement hydration, alkali degradation of cellulosic fibers) – although

* Corresponding author.
E-mail address: ricardo.serpell@hefr.ch (R. Serpell).

https://doi.org/10.1016/j.conbuildmat.2022.128392
Received 25 November 2021; Received in revised form 27 June 2022; Accepted 3 July 2022
Available online 21 July 2022

methods to identify and deal with them are available [9,12]. For cast-in-place applications, however, the most challenging aspect of WCC is their high drying shrinkage. Due to the large water absorption capacity of lignocellulosic materials, WCC demand a large amount of water to reach the required pourability. Immediately after casting, the material begins to lose moisture, shrinking as bound water leaves the saturated fibers. In unrestrained elements, shrinkage leads to significant dimensional changes over time, which complicates construction planning. If subject to external restraints, tensile stresses develop leading to cracking.

Just as in conventional concrete, an aggregate skeleton can provide an internal constraint to drying shrinkage of WCC. Harder, less absorbent lignocellulosic agricultural wastes, such as shell bits and seeds, used as aggregates have been shown to reduce shrinkage of WCC [7]. Notably, since aggregates are the bulk of the material, their characteristics largely determine the properties of the whole composite. Hence, shifting the WCC from the matrix phase to the aggregate phase of the material could be an effective strategy to develop a timber-compatible lightweight concrete. Pre-fabricated WCC-based LWA would have hardened and shrank before use. Lightweight concretes made with them would benefit from the properties of WCC with higher control over shrinkage, while their production would still provide a viable option for the reuse of wood wastes and probably other construction and demolition fines.

Cold bonding can be a viable, low-energy option for the production of artificial LWA with these materials. Unlike methods requiring autoclaving or sintering at high temperature, production of aggregates by cold bonding relies on hardening reactions that take place spontaneously at ambient temperature [13]. The process involves the agglomeration of fine particles into pellets by the combined action of tumbling forces and capillary forces in a rotating vessel where the raw materials are brought into contact with the right amount of moisture [14]. The freshly made pellets maintain their shape due to these forces, but can gain additional strength by chemical reactions involving binders included in the raw material mix or in the added liquid. Most recent research has focused on the pelletization of ashes from coal fired power plants, in many cases as a means to obtain an intermediate product for the production of sintered aggregates [15–18]. Since cold bonded aggregates are significantly weaker than sintered aggregates, some researchers have explored the use of chemical activators to improve the mechanical strength of fly- and bottom-ash based pellets [19,20]. Few researchers report attempts to pelletize alternative raw materials and, in general, these are considered as additions to fly-ash–cement mixtures (e.g. [21,22] on the use of ashes from municipal solid waste incinerators). Cold bonded fly-ash LWA are also denser than most sintered LWA. Several methods have been tried to obtain a lighter product, including using hydrogen peroxide as a foaming agent [23] or incorporating powdered expanded perlite in the raw materials using a two-step pelletization process to encapsulate the mixture in a harder, cement-rich shell [24]. The two-step process is particularly appealing in the context of lightweight concrete for timber construction, as it allows encapsulation of functional additions, such as phase changing materials that can be used to fine-tune the thermal performance of the composite [25]. The two-step process was found to enhance physical and mechanical properties and reduce leachates from the pellets.

No reference to cold bonding of wood sawdust or wood ashes could be found in the literature review. As wood consumption continues to increase – partly due to population growth and partly due to increased use as a substitute for more energy intensive construction materials –, larger amounts of wood waste need to be dealt with. Although recycling and energy recovery from wood waste allow the conservation of primary resources [26], the former is challenging due to the variability of the waste, and the latter leads to the production of wood ashes, a potentially dangerous secondary waste. Aggregate production has been identified as a potential use for current and future ashes [27]. Wood ashes, both from grate and fluidized bed combustion, have been found to be partially hydraulic, setting and hardening under water, although only when intermixed with Portland cement [28]. Their use can lead to cold bonded aggregates requiring less cement to achieve target mechanical properties with positive impact on the potential environmental performance of the cold-bonded LWA.

The reported research was aimed at exploring the feasibility of producing LWA by cold bonding of locally-sourced biomass waste (wood sawdust and wood ashes). The exploration included an empirical assessment of the effects of raw material proportion adjustments on relevant properties of the LWA. The assessment was intended to provide knowledge on effective ways to achieve target properties with the specific set of materials and processes studied, and also to provide insights on the performance potential of this new type of LWA.

2. Materials and methods

The exploratory research was organized in three consecutive empirical campaigns. The first was aimed at identifying controllable factors of the production process (i.e. material proportions and cold-bonding parameters), and was based on trial experiments where single factors were serially adjusted. The second was aimed at modeling the relationship of factors and relevant responses of the aggregates, and was based on a factorial experiment designed according to response surface methodology. The third was aimed at validating the findings and expanding the experimental region explored in the factorial experiment, and was based on trial experiments at combinations of factor levels defined according to previous results.

2.1. Raw materials

In order to cover a wider range of particle sizes and achieve higher particle packing, two sawdust sources were used. Coarse sawdust of spruce (*Picea abies*) wood was sourced from a nearby timber mill (in Treyvaux, canton Fribourg, Switzerland). The coarse sawdust was sieved with a 2.00 mm mesh to obtain a more homogeneous raw material, discarding larger particles and shavings present in it. Stocked in the lab, its moisture content equilibrated at 17.7% by dry weight. At this moisture content, the particle density of the coarse sawdust was estimated at 0.415 g/cm^3 based on reference values for the air-dried density (12% moisture) and volumetric shrinkage (green to oven-dry) of spruce wood [29,30]. Uncompacted bulk density at the stock moisture content was measured at 178 kg/m^3. Fine sawdust, also known as wood dust, was obtained from the vacuum filter stacks of sanding machines in the campus model-making workshop, which are mostly used to sand pieces of Medium-Density-Fiberboard (MDF). This very fine material exhibited a moisture content of 6.1% and an uncompacted bulk density of 254 kg/m^3. Dry-sieving showed it to be comprised of fibers under 0.5 mm in size.

Wood ashes were sourced from a thermal-energy supplier in canton St. Gallen, Switzerland. The ashes are a powdered inorganic residue from wood combustion, and are comprised mostly of basic oxides of Calcium and other metals. They were sieved with a 0.5 mm mesh to discard contamination (small stones, sand, aggregated particles) and to obtain a finer and more homogeneous material. The retention rate (i.e. amount of material passing the sieve) was 60% by weight. The ashes exhibited a particle density of 2,630 g/cm^3 (measured by water pycnometry, assuming non-porous particles). The two sawdust sources and the wood ashes can be seen in Fig. 1 together with two examples of pellets obtained from them.

In addition to the previously mentioned raw materials, all formulations included hydraulic cement, assimilable to type CEM II/B (65 to 94% cement clinker plus supplementary cementitious materials). Preliminary trial batches also explored the use of finely ground limestone filler (calcium carbonate). Tap water was used in all cases.

The particle size distribution (PSD) of the raw materials is shown in Fig. 2. The PSDs of the finer materials were measured by laser diffraction with a Malvern Mastersizer 3000E particle size analyzer, using water

Fig. 1. Main raw materials (besides Portland cement) and two examples of pellets obtained from different raw material mixture formulations.

(for sawdust and ashes) or reagent grade isopropyl alcohol (for cement) as dispersants. The coarse sawdust PSD was measured by dry sieving. As seen in Fig. 2, cement was the finest material (D50 = 16.5 μm), followed by fine sawdust (D50 = 47 μm), and wood ashes (D50 = 70 μm). Coarse sawdust sizes extended up to 2.0 mm (D50 = 1.06 mm).

2.2. Pelletizing equipment

A rotating drum pelletizer (Eirich) was used throughout the reported research (Fig. 3). This laboratory-sized machine is equipped with a flat bottom drum of 1.0 m diameter and 0.25 m depth. The angle and speed of the drum can be varied continuously during operation by electronic means, between 25° and 95° from the horizontal, and between 0.15 m/s and 2.30 m/s (drum wall speed, equivalent to 2.6 – 43.8 rpm), respectively. At the uppermost part of the drum a fixed blade scraps the drum side surface, but there is a clearance of about 1 cm between this blade and the bottom surface of the drum. A motorized rotating scrapper arm can be activated to improve separation of material from the bottom surface of the drum. Liquids can be incorporated through two spraying nozzles fixed to the drum cover. In addition to the standard-equipment ball valves that control each nozzle, a gate valve was added at the main inlet to limit water flow-rate. The flow-rate was measured daily, before starting the production of pellets.

2.3. Pelletizing process

Pellets were produced in batches of approximately 5.0 L each (solids, particle volume). Raw materials' masses proportioned according to the formulations prescribed in the experimental plan were adjusted to match the target volume. Solid raw materials were weighed to the nearest 1%. Water was dosed by nozzle-valve open-time, calibrated using the measured flow-rate.

At the start of each batch, the dry pelletizer drum was set at its lowest angle (25° from horizontal) and lowest rotation speed, with the rotating scrapper arm turned on. Raw materials were roughly mixed in an external container and then incorporated into the slow-rotating drum. A scrapper was used to aid the mixing of the dry materials. After 3 min the drum inclination was increased to 50°, simultaneously increasing its speed until the dry material was observed to roll on the drum surfaces. Rolling was achieved in most cases at about 0.8 m/s. At this point, 2/3 of the water prescribed in the corresponding formulation was added. The then humid precursor material was reworked manually while rolling in the drum in order to homogenize it, destroying any pellets that had formed during the addition of initial water. This homogenization step was carried out for approximately 3 min. Drum angle was then increased to 55° to achieve continuous rolling of the material. Additional water was added in doses of about 100 ml, adjusting drum angle and speed to keep material rolling (i.e. keeping the material falling back to the

Fig. 3. Rotating drum pelletizer used in the reported study.

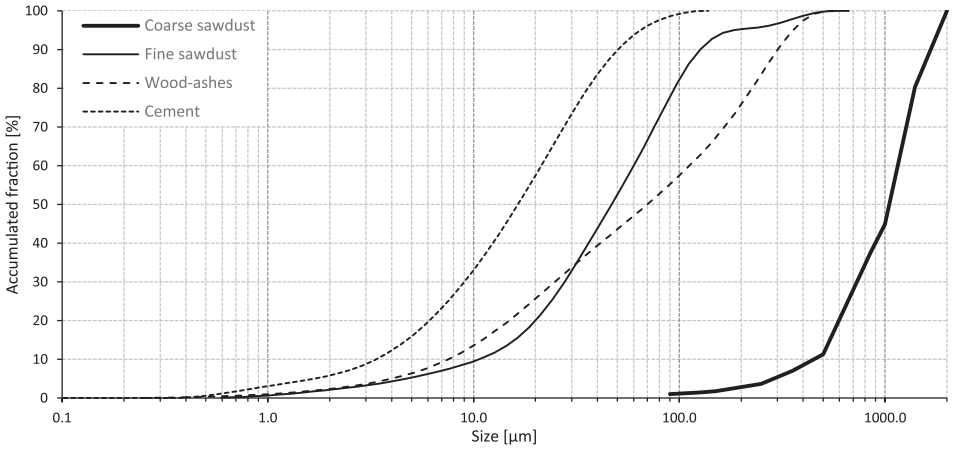

Fig. 2. Particle size distributions of raw materials: coarse sawdust (dry sieving), fine sawdust and wood-ashes (laser diffraction in water), and cement (laser diffraction in isopropyl alcohol).

bottom of the drum before hitting the upper scrapper blade). As soon as pellets were observed to start forming again, no more water was added, since required moisture for balling had been achieved. The material was kept rolling in the drum for 10 additional minutes to allow further agglomeration and densification of the pellets. Depending on the formulation, optimal drum angle and rotation speed during this final stage varied between 55° and 60°, and between 0.9 and 1.0 m/s. Some formulations called for a part or all of the cement dose to be added at the end of the process to coat the pellets. In those cases, the cement was sprinkled over the rolling pellets 2 min before the end of the densification stage. On average, the production of a batch took 25 min from raw material charging to pellet discharging.

Pellets were discharged into a plastic container by increasing the angle of the rotating drum to 95°. The obtained pellet batch was weighed and its mass compared to the weight of the dry raw materials to estimate its final water content (i.e. water demanded for the pelletization of the specific formulation of raw materials). Pellets were then transferred to covered plastic containers and stored inside the lab (climatized room, at ~ 20 °C) until the date of testing.

2.4. Testing of pellets

Testing of pellets started 7 days after production and included particle size gradation, particle crushing strength, particle density, water absorption capacity and drying shrinkage. Particle size gradation was performed by sieving using mesh opening sizes 16.0, 11.2, 8.0, 5.6 and 4.0 mm. In some cases, pellets had bonded superficially and had to be manually disaggregated prior to sieving. The apparent stickiness of the material was recorded qualitatively on a 0 to 2 scale. Strongly bonded batches required significant force to separate them. Fortunately, individual pellets were not damaged in the process as they were also very strong in these same batches (these observations are discussed in more detail in section 4). A fineness index was constructed as a quotient of summed cumulative fractions below and above 8.0 mm size, eq. (1), where: $f_{acc.i}$ is the cumulative weight fraction of particles passing the sieve of size i. The resulting fineness index ranges between 0 (all particles larger than 8.0 mm) and 1 (all particles smaller than 8.0 mm).

$$F = (f_{acc.4.0} + f_{acc.5.6} + f_{acc.8.0}) \; / \; (f_{acc.11.2} + f_{acc.16.0} + \; 1) \tag{1}$$

A sample of 500 g of pellets sized between 11.2 mm and 8.0 mm was taken to be used for the measurement of particle crushing strength, particle density, water absorption capacity, and drying shrinkage. The goal of sampling only a narrow band of particle sizes was to reduce dispersion of test results within each pellet batch. Single particles were tested in compression at 7 and at 70 days after production (latest date within project planning constraints) using an electromechanical press equipped with a 1 kN load cell, in deformation-controlled mode. Particle crushing strength σ in MPa was calculated from Eq. (2) [13], where P is the failure load (N) and d is the distance between the loading plates (mm). Values reported in the section 4 are the medians and coefficients of variation of 6 tests per batch per date.

$$\sigma \approx \; 2.8P/\pi d^2 \tag{2}$$

Particle density and water absorption capacity were determined following procedures similar those specified for coarse aggregates in EN 1097–6 [31]. A sample of 300 g of pellets was brought to Saturated Surface Dry (SDD) condition after being immersed for 48 h. The solids volume of the SSD sample was determined using a 2-liter capacity pycnometer. The sample was then oven dried at 105 °C for 72 h to determine its dry mass. The measured SSD densities and water absorption capacities were used to estimate the output volume of the pelletization process according to eq. (3):

$$V_{out,\ SSD} = \; (\; WAC \; (M_{out} - - \; M_w) \; + \; M_{out} - - \; M_w \;) \; / \; D_{SSD} \tag{3}$$

where, $V_{out,\ SSD}$ is the output volume of the pelletization process in SSD condition, WAC is the water absorption capacity of the pellets, M_{out} and M_w are the total mass output of the pelletization process and the mass of water added to it, respectively, and D_{SSD} is the particle density of the pellets in SSD condition. The estimated output volume was then used to estimate the resulting cement content of each formulation (mass of cement dose per solid volume of pellets in SSD condition).

A rough measurement of the solids volume of the oven-dried pellets was performed by placing the sample back in the pycnometer and filling it with water to the afore mark within 15 s. Although this method has limited validity for highly porous particles, it was considered sufficient to estimate the relative drying shrinkage of the different pellets.

3. Experimental program

3.1. Preliminary trials: Selection of factors and definition of factor level ranges

Preliminary tests were carried out to identify factors that can be effectively controlled and to determine plausible level ranges for them (upper and lower limits). Coarse and fine sawdust, calcium carbonate, wood ashes and cement were used as raw materials. Their initial proportions were established by trial and error and then varied to explore the feasibility limits of the pelletization process.

Ideally, raw material mixtures should contain between 60% and 90% of particle sizes below 40 μm to achieve the degree of fineness required for proper pelletization [32]. In the initial trials, larger doses of finer materials (e.g. filler, cement) increased cohesiveness and allowed formation of smaller and better shaped pellets. However, due to the large coarse sawdust doses used, none of the mixtures had more than 40% of particles under 40 μm. Cement doses were kept below 300 kg/m^3 of solids. At this level, the contribution of cement to the cohesivity of the mixture was small compared to the contribution of the much larger dose of filler (calcium carbonate or wood ashes). Wood ashes were observed to provide sufficient cohesivity in place of the calcium carbonate initially considered. Despite its small particle size, the contribution of fine sawdust to the cohesivity of the raw mixture could not be clearly established from the preliminary test results. Trials incorporating a large fraction of fine sawdust still resulted in large pellets. Most likely, the densification that takes place due to gravity forces acting on the raw mixture was reduced due to the very low density of the fine sawdust particles.

Due to the widely different hygroscopicity and water absorption capacity of the different raw materials, the amount of water required to form the pellets varied according to their proportion. Water demand was significantly higher at high sawdust contents, with coarse sawdust having a slightly larger effect. As a consequence, the water dose could not be treated as an independent variable. Likewise, the drum angle and rotation speed of the pelletizer had to be continuously adjusted to maintain proper rolling of the raw mixture according to its physical properties (density, fineness, moisture content, etc.). As a result of these observations, it was decided to focus further exploration on the effects of the raw materials' ratios on the properties of the resulting pellets. Raw materials selected were: coarse and fine sawdust, wood ashes and cement.

In order to reduce the number of independent factors, it was decided to use a fixed cement dose. On the one hand, the expected effects of the cement dose on the properties of the pellets are relatively known: a larger cement dose is expected to facilitate production of smaller pellets (due to the small particle size of cement), increase long-term strength of the pellets (due to cement hydration processes), and increase the particle density of the pellets (due to the higher particle density of cement compared to other fines). On the other hand, the relative effects of other factors were not expected to depend significantly on the cement dose. Ultimately, the goal of the factorial exploration was to determine if optimal combinations of factor levels exist that maximize relevant pellet properties at any given cement dose.

The following raw materials' volumetric ratios were selected as independent factors:

X1: $\boldsymbol{Bc/B} = Bc/(Bc + Bf)$: The ratio of coarse sawdust to total sawdust in the raw mixture (i.e. sawdust coarseness), with *Bc*: volume of coarse sawdust, *Bf*: volume of fine sawdust, and *B*: total volume of sawdust ($Bc + Bf$). For the purpose of proportioning, it was assumed that both sawdust sizes had comparable particle densities.
X2: $\boldsymbol{B/S} = B/(B + A + c)$: The ratio of sawdust to total solids in the raw mixture (i.e. the sawdust content), with *S*: total solids volume of the raw mixture, comprised of *B*: total volume of sawdust, *A*: volume of wood ashes, and *c*: volume of cement included in the raw mixture.
X3: $\boldsymbol{c/C}$: The fraction of the cement dose included in the raw mixture, with *C*: volume of the total cement dose, and *c*: volume of cement intermixed with the raw materials. When this fraction is<1, the rest of the cement dose is added at the end of the process as a coating to the already formed pellets.

A graphical key to the expected composition of the resulting pellets is shown in Fig. 4. In the freshly made pellets, voids between particles are partly filled with water. The coating is formed only when a fraction of the cement dose is added at the end of the process, when pellets have already formed and densified. According to observations from the trial tests, it was decided that sawdust coarseness would be explored in the range 0.25 to 0.75 coarse to total sawdust ratio, sawdust contents would be explored in the range 0.40 to 0.60 sawdust to total solids ratio, and the fraction of the constant cement dose included in the raw mixture would range from 0 (all cement as a coating to the pellet) to 1 (all cement in the bulk of the pellet). The targeted constant cement content was fixed at 240 kg/m^3 of solids (particle volume).

3.2. Experimental design and raw material mix formulations

A response surface approach was chosen to explore the experimental region defined by the selected ranges of factor levels. This approach allows the identification of response maximums/minimums within the experimental region, making use of experimental designs that enable the estimation of the second order effects of the factors in addition to their linear effects and interactions. The selected Box-Behnken experimental design [33] is a proficient tool for this purpose, requiring only three levels for each factor. The 3-factor version of this design is comprised of 13 different factor-level combinations (cases), including a central one at the middle level of all factors. By replicating this central case 4 times, the design can be separated in four equivalent blocks (i.e. each having a balanced combination of factor levels), simplifying the practical execution of the experiment.

The full experimental design, including coded and empirical levels of the factors and the raw materials' formulation for each case is shown in Table 1. The total volume of raw materials required for each 5.0 L batch was determined deducting the estimated volumes of the coating and of the voids from the total volume of the batch. The volume of the coating was estimated as the solid volume of cement plus the volume of water binding the cement particles. The volume of voids was estimated based on an empirical regression of water uptake observed in the preliminary tests, as: $15\% + B/S \cdot 40\% + Bc/B \cdot 7.5\%$. These estimations were meant to approach as much as possible the target batch volume, but the actual volume obtained was later determined based on the output weight and the resulting particle density of the pellets. As seen in Table 1, the experiment was executed in four blocks. The four batches comprising each block were produced on a single day in random order. The four blocks were completed within one week. Tests on pellets from a given block were also performed on a single day at fixed time intervals after production.

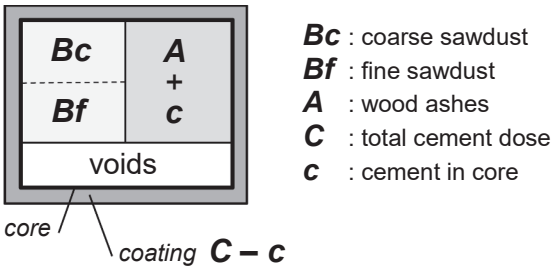

Fig. 4. Scheme of pellet composition.

4. Results and discussion

4.1. General observations

Results from all individual cases in the factorial experiment are shown in execution order in Table 2. An additional central case batch (17c) was produced in the 4th block to test within-block variability.

The amount of water required to form the pellets was generally larger than the voids volume predicted in the formulations. Water demand was 14% larger on average, but the difference was seen to depend on the coarseness of the sawdust, with cases at higher contents of fine sawdust demanding on average 31% more water than predicted, and cases at higher contents of coarse sawdust demanding on average only 1% more. As a result, batch output mass was larger than predicted.

Concurrently, output volumes, – estimated from the output mass and the measured particle density of the pellets –, were 10% lower on average than the 5-liter target, yet varying significantly between cases, according to sawdust content and sawdust coarseness. The smaller and variable output volumes resulted in correspondingly higher and variable effective cement contents. However, as will be discussed in section 4.4, variations in effective cement content did not correlate with observed variations in the particle crushing strength of the pellets.

Pellet properties were observed to vary significantly among cases. In the following sections, these variations are explained in relation to the raw materials ratios on the basis of factor-response regression models. The significance of the models and of the model coefficients (factor effect estimates) was tested using analysis of variance (ANOVA). In general, a significance level of 5% (p-value < 0.05) was used to identify statistically significant effects. Nevertheless, some effects having slightly larger p-values are also discussed when their estimated coefficients were relatively large. Owing to the normalization of factor levels in the regression model, the absolute magnitude of the effect coefficients can be considered a good indicator of their relative importance.

4.2. Superficial bonding (stickiness) and particle size distribution (fineness)

Seven days after production, the freshly made pellets exhibited different degrees of superficial bonding during storage. As seen in Table 2, within the 17 cases in the experiment, 6 (35%) exhibited significant bonding (qualitative value ≥ 1.0). The ANOVA of the stickiness response model (Table 3) shows that experiment factors can only partially explain the observed differences (model $p = 0.135$). Sawdust coarseness, *Bc/B*, was the only factor displaying a significant effect on the response. According to the corresponding coefficient, superficial bonding of freshly made pellets during storage increases when the coarse sawdust ratio is increased. Although not achieving the required significance level, the second order effect of *Bc/B* exhibited the second largest coefficient. This second order effect would indicate that bonding increases in a curvilinear way as the coarse sawdust ratio is increased. In pellets made from raw material mixes at higher coarse sawdust ratios, particle surfaces were rougher due to coarse sawdust particles protruding from them. In storage, these particles are in contact with each other. Capillary forces develop between the wet fibrous surfaces of the sawdust particles, bringing them in closer contact as the freshly made

Table 1
Factorial experimental design, factor levels and corresponding pellet formulations.

		Formulations for 5.0 L batches														
		Factors						Estimated volumes				Raw materials masses				
		Coded levels			Empirical levels			Coating	Core			Coating	Core			
		X1	X2	X3	X1	X2	X3	total[1]	total	voids[2]	solids	cement	coarse s.	fine s.	ashes	cement
Case	Block				*Bc/B*	*B/S*	*c/C*	[L]	[L]	[L]	[L]	[kg]	[kg]	[kg]	[kg]	[kg]
1	3	−1	−1	0	0.25	0.40	0.50	0.26	4.74	1.56	3.18	0.60	0.13	0.40	4.51	0.60
2	2	+1	−1	0	0.75	0.40	0.50	0.26	4.74	1.74	3.00	0.60	0.37	0.12	4.23	0.60
3	4	−1	+1	0	0.25	0.60	0.50	0.26	4.74	1.94	2.80	0.60	0.17	0.52	2.44	0.60
4	1	+1	+1	0	0.75	0.60	0.50	0.26	4.74	2.11	2.62	0.60	0.49	0.16	2.25	0.60
5	2	−1	0	−1	0.25	0.50	0.00	0.52	4.48	1.65	2.83	1.20	0.15	0.44	3.72	0.00
6	4	+1	0	−1	0.75	0.50	0.00	0.52	4.48	1.82	2.66	1.20	0.41	0.14	3.50	0.00
7	1	−1	0	+1	0.25	0.50	1.00	0.00	5.00	1.84	3.16	0.00	0.16	0.49	3.13	1.20
8	3	+1	0	+1	0.75	0.50	1.00	0.00	5.00	2.03	2.97	0.00	0.46	0.15	2.89	1.20
9	1	0	−1	−1	0.50	0.40	0.00	0.52	4.48	1.56	2.92	1.20	0.24	0.24	4.61	0.00
10	3	0	+1	−1	0.50	0.60	0.00	0.52	4.48	1.91	2.56	1.20	0.32	0.32	2.70	0.00
11	4	0	−1	+1	0.50	0.40	1.00	0.00	5.00	1.74	3.26	0.00	0.27	0.27	4.13	1.20
12	2	0	+1	+1	0.50	0.60	1.00	0.00	5.00	2.14	2.86	0.00	0.36	0.36	1.99	1.20
13	1	0	0	0	0.50	0.50	0.50	0.26	4.74	1.84	2.90	0.60	0.30	0.30	3.31	0.60
14	2	0	0	0	0.50	0.50	0.50	0.26	4.74	1.84	2.90	0.60	0.30	0.30	3.31	0.60
15	3	0	0	0	0.50	0.50	0.50	0.26	4.74	1.84	2.90	0.60	0.30	0.30	3.31	0.60
16	4	0	0	0	0.50	0.50	0.50	0.26	4.74	1.84	2.90	0.60	0.30	0.30	3.31	0.60

[1] Coating volume estimated considering 0.2 g of water per gram of cement
[2]Volume of voids estimated from regression of preliminary test results: 15% + *B/S*·40% + *Bc/B*·7.5%

pellets partially desiccate. This likely results in strong interlocking forces between the fibers and lignin in contacting surfaces, bonding exposed sawdust particles and, by extension, the pellets that they coat. Pellet surfaces exposing particles of finer sawdust did not bond, likely due to resins used in the production of MDF partially or totally covering the fibers in the sawdust.

Large differences in the size distribution of the pellets were also observed among cases. Formulations at higher contents of coarse sawdust were observed to produce distinctly larger pellets. According to the ANOVA (Table 4), the fineness model only partially explains the observed differences (model $p = 0.295$). In agreement with direct observations, the ANOVA shows that sawdust coarseness, *Bc/B*, had a significant effect on the response. According to the corresponding coefficient (−0.131), the fineness of the pellets decreases when the coarse sawdust ratio is increased. Although not reaching required significance level, the fraction of the cement dose intermixed with the raw materials, *c/C*, exhibited the second largest effect coefficient (0.093), indicating that fineness would increase as more of the cement is intermixed. Both effects relate to the contribution of each specific material to the particle size distribution of the raw material mix. As seen in Fig. 5(a), as the coarse sawdust ratio increases, the particle size distribution of the raw material mix shifts to larger average sizes. As seen in Fig. 5(b), this results in the formation of larger pellets. Due to relatively weaker bonding forces between larger particles the shift towards larger particle sizes also reduces the pellet outcome of the process, because larger pellets are harder to form and are less stable (e.g. less resistance to inter-particle impact) [32].

4.3. Particle density, water absorption capacity and drying shrinkage

Large differences in SSD and dry densities were observed among cases. At 7 days after production, particle densities in SSD condition ranged from 1.591 to 1.834 g/cm^3, and from 1.254 to 1.771 g/cm^3 in oven-dry condition. These values are significantly lower than those reported for pure fly-ash cold-bonded pellets (ranging from 1.650 to 2.120 g/cm^3 [14]) and close to those reported for agricultural wastes used as aggregates, such as coconut shells (ranging from 1.120 to 1.890 g/cm^3 [14,34,35]). Formulations at higher sawdust contents exhibited lower densities. As seen in the ANOVA (Table 5), sawdust content had a significant effect on both SSD and dry density. According to the corresponding model coefficients, the particle density of the pellets decreases when the content of sawdust, *B/S*, is increased. In the range of sawdust contents explored, SSD and dry densities decrease 4.0% and 4.8%, respectively, per each 10% increase in sawdust content with respect to the average density at 50% sawdust.

The ANOVA further indicates that both, SSD and dry density, were also significantly affected by sawdust coarseness, *Bc/B*. Sawdust coarseness exhibited a significant second order effect on SSD particle density, but no first order effect. According to the response model, SSD density reaches a maximum at around 0.5 coarse sawdust ratio, decreasing at either side of this value. Conversely, sawdust coarseness exhibited a significant first order effect on dry particle density, but its second order effect did not reach the required significance level. According to the first order effect coefficient – the largest in the dry density response model –, the dry density of the pellets decreases when the coarse sawdust ratio is increased. These first and second order effects on density could be explained by changes in the bulk density of the sawdust mix. Considering the properties of the sawdust sources used, bulk density of the sawdust mix is expected to decrease as coarse content increases. However, improved particle packing, as the sawdust mix approaches a specific optimal coarse-to-fine ratio, would result in a non-linear change. In the case of SSD particle density, the first order effect of sawdust coarseness could be compensated by the combined effects of mass gain and volumetric expansion due to water absorption. As will be discussed later in this section, formulations with lower coarse sawdust ratios produced pellets exhibiting higher water absorption capacities and larger drying shrinkages (therefore, larger volumetric expansions due to water uptake). If the volumetric expansion would grow faster than the mass gain in SSD condition, a net decrease in SSD density would result as sawdust coarseness decreases.

Despite not reaching the required significance level in the ANOVA, response model coefficients indicate that the dry density of the pellets might be affected by the fraction of the cement dose incorporated in the raw materials, *c/C*, increasing when the cement fraction is increased, particularly at high sawdust contents (interaction *B/S·c/C*). Such effects are expected due to the contribution of small cement particles to the packing efficiency of the raw material mix. The interaction effect could be due to cement content variations having a relatively larger effect when ash contents are lower as a result of higher sawdust contents.

The ANOVA of the dry density model also shows that the response

Table 2
Experimental results.

					Production				Pellet properties										
		Factors			Water	Output		Cement			Density (mass/volume)			W. abs.	Drying	Crushing strength			
		X1	X2	X3	uptake*	mass	volume	dose**	Fineness	Stickyness	ssd/ssd	dry/ssd	dry/dry	capacity	shrinkage	7d	C.V.	70d	C.V.
Case	Blk.	*Bc/B*	*B/S*	*c/C*	[L/kg]	[kg]	[cm^3]	[kg/m^3]	[–]	[–]	[g/cm^3]	[g/cm^3]	[g/cm^3]	[% dry m.]	[% sat.v.]	[MPa]	[%]	[MPa]	[%]
1	3	−1	−1	0	0.33	8.45	5,065	237	0.52	0.00	1.734	1.255	1.771	38.2	29.1	0.029	39	0.049	62
2	2	+1	−1	0	0.31	8.00	4,596	261	0.28	1.00	1.742	1.329	1.560	31.1	14.8	1.121	21	1.506	25
3	4	−1	+1	0	0.51	7.00	4,385	274	0.22	0.00	1.623	1.058	1.660	53.4	36.3	0.047	13	0.061	21
4	1	+1	+1	0	0.46	6.35	4,036	297	0.09	2.00	1.591	1.081	1.254	47.1	13.7	0.624	17	1.288	15
5	2	−1	0	−1	0.42	7.85	4,882	246	0.50	0.00	1.633	1.134	1.557	44.0	27.2	0.020	33	0.042	64
6	4	+1	0	−1	0.37	7.25	4,359	275	0.08	2.00	1.685	1.211	1.427	39.2	15.1	0.568	24	0.999	40
7	1	−1	0	+1	0.44	7.75	4,972	241	0.60	0.00	1.610	1.084	1.545	48.5	29.8	0.049	47	0.069	13
8	3	+1	0	+1	0.36	6.95	4,374	274	0.34	1.00	1.610	1.168	1.552	37.9	24.7	1.379	14	0.442	11
9	1	0	−1	−1	0.36	8.60	5,014	239	0.24	1.00	1.742	1.258	1.577	38.5	20.2	0.084	146	0.488	115
10	3	0	+1	−1	0.45	6.65	4,167	288	0.23	0.00	1.635	1.099	1.461	48.8	24.8	0.022	25	0.060	142
11	4	0	−1	+1	0.32	8.10	4,413	272	0.42	0.50	1.834	1.395	1.690	31.5	17.5	1.466	24	1.868	28
12	2	0	+1	+1	0.46	6.45	3,960	303	0.43	0.00	1.661	1.117	1.658	48.7	32.6	0.072	31	0.082	24
13c	1	0	0	0	0.41	7.50	4,691	256	0.13	0.50	1.661	1.136	1.587	46.3	28.5	0.044	55	0.555	106
14c	3	0	0	0	0.39	7.40	4,449	270	0.47	0.00	1.708	1.198	1.711	42.6	30.0	0.171	125	0.714	82
15c	4	0	0	0	0.39	7.40	4,398	273	0.26	0.00	1.713	1.211	1.685	41.4	28.1	0.092	52	0.629	82
16c	2	0	0	0	0.38	7.35	4,152	289	0.28	1.00	1.751	1.283	1.500	36.4	14.5	0.333	55	1.449	28
17c	4	0	0	0	0.37	7.45	4,363	275	0.20	0.00	1.736	1.246	1.653	39.4	24.6	0.099	36	0.687	87
All-case average					0.40	7.44	4,487	269	0.31	0.53	1.686	1.192	1.579	41.9	24.2	0.366	45	0.658	73
All-case std. deviation					0.06	0.67	347	20	0.16	0.70	0.067	0.097	0.127	6.5	7.2	0.506	37	0.608	78
Central-case average					0.39	7.42	4,411	272	0.27	0.30	1.714	1.215	1.627	41.2	25.1	0.148	65	0.807	87
Central-case std. dev.					0.01	0.06	193	12	0.13	0.45	0.034	0.055	0.085	3.7	6.3	0.113	35	0.364	29

* Added water to raw materials' mass ratio
** Effective cement dose per m^3 of solid volume estimated from output mass and pellet particle density in SSD condition

Table 3
ANOVA: stickiness.

Source	*Coefficient* [*]	*SS*	*df*	*MS*	*F*	*p*
Model		6.248	10	0.625	2.52	0.135
intercept	0.542	0.44	1	0.440	1.775	0.231
block	−0.086	0.125	1	0.125	0.505	0.504
Bc/B	**0.750**	4.5	1	4.500	18.153	**0.005**
B/S	−0.062	0.031	1	0.031	0.126	0.735
c/C	−0.187	0.281	1	0.281	1.135	0.328
Bc/B · B/S	0.207	0.162	1	0.162	0.652	0.450
Bc/B · c/C	−0.250	0.25	1	0.250	1.009	0.354
B/S · c/C	0.039	0.005	1	0.005	0.02	0.893
$(Bc/B)^2$	0.400	0.668	1	0.668	2.696	0.152
$(B/S)^2$	0.025	0.003	1	0.003	0.01	0.923
$(c/C)^2$	0.025	0.003	1	0.003	0.01	0.923
Residuals		1.487	6	0.248		
Corr. Total		7.735	16			

* qualitative units (see section 2.4)

Table 4
ANOVA: gradation fineness.

Source	*Coefficient* [*]	*SS*	*df*	*MS*	*F*	*p*
Model		0.281	10	0.028	1.589	0.295
intercept	0.287	0.123	1	0.123	6.977	0.038
block	−0.007	0.001	1	0.001	0.042	0.844
Bc/B	**−0.131**	0.138	1	0.138	7.800	**0.031**
B/S	−0.061	0.030	1	0.030	1.699	0.240
c/C	0.093	0.068	1	0.068	3.874	0.097
Bc/B · B/S	0.024	0.002	1	0.002	0.125	0.736
Bc/B · c/C	0.040	0.006	1	0.006	0.362	0.569
B/S · c/C	−0.002	9E-06	1	9E-06	0.001	0.983
$(Bc/B)^2$	0.029	0.003	1	0.003	0.196	0.674
$(B/S)^2$	−0.021	0.002	1	0.002	0.107	0.755
$(c/C)^2$	0.081	0.028	1	0.028	1.564	0.258
Residuals		0.106	6	0.018		
Corr. Total		0.387	16			

* arbitrary units (see section 2.4).

was affected by the execution date (as seen in the significance level of the "block"). According to the corresponding coefficient, oven-dry density tended to increase as the experiment progressed. This effect could be due to operator influence during pellet production (e.g. improving pellet densification as subsequent batches were produced), although a similar effect on SSD density should be seen. Further experiments would be required to identify the real source of the variation.

Whereas water absorption capacity of the pellets was mostly affected by sawdust content, drying shrinkage was most affected by the coarseness of the sawdust. The ANOVA of the water absorption model (Table 6) shows that sawdust content, *B/S*, had a significant effect on the response. According to the corresponding model coefficient, the water absorption capacity of the pellets increases when the sawdust content is increased. On the other hand, sawdust coarseness, *Bc/B*, is seen to have a significant opposite effect on the response: water absorption capacity of the pellets decreases when the coarse sawdust ratio increases. Accordingly, at any given sawdust content, water absorption capacity would be minimum if only coarse sawdust is used.

The ANOVA of the drying shrinkage response model (also in Table 6) shows that the factors can only partially explain the observed variations (model $p = 0.266$). The ANOVA shows that sawdust coarseness, *Bc/B*, was the only factor with a significant effect on the response. According to the corresponding coefficient, drying shrinkage of the pellets decreases when the coarse sawdust ratio is increased. Although sawdust content, *B/S*, was also expected to affect drying shrinkage, in the range of contents explored its effect did not reach the required significance level. Its *p*-value was nevertheless the second smallest in the ANOVA.

4.4. Particle crushing strength

The particle crushing strength of the pellets varied widely among cases, ranging between 0.02 and 1.40 MPa at 7 days after production and between 0.05 and 1.87 MPa at 70 days. These values compare favorably with results from expanded clay aggregates: failure loads for similarly sized (9 mm) particles tested in uniaxial compression ranged from 75 to 130 N [36], which translates to 0.83 to 1.43 MPa using equation (2). The ANOVA of the 7-day strength model (Table 7) shows that all main factors had a significant effect on the response. According to the corresponding model coefficients, 7-day strength increases when the coarse sawdust ratio, *Bc/B*, is increased and/or when the fraction of the cement dose incorporated in the raw material mix, *c/C*, is increased, but decreases when sawdust content, *B/S*, is increased. The ANOVA results also show a significant interaction effect between the sawdust content and the fraction of the cement dose incorporated in the raw material mix (*B/S·c/C* interaction), indicating that their effects are mutually dependent. According to the corresponding coefficient, at lower sawdust contents, 7-day strength is positively affected by increasing the fraction of cement incorporated in the raw materials (same sign interaction, adding to first order effect), whereas at higher sawdust contents, 7-day strength remains largely unaffected by it

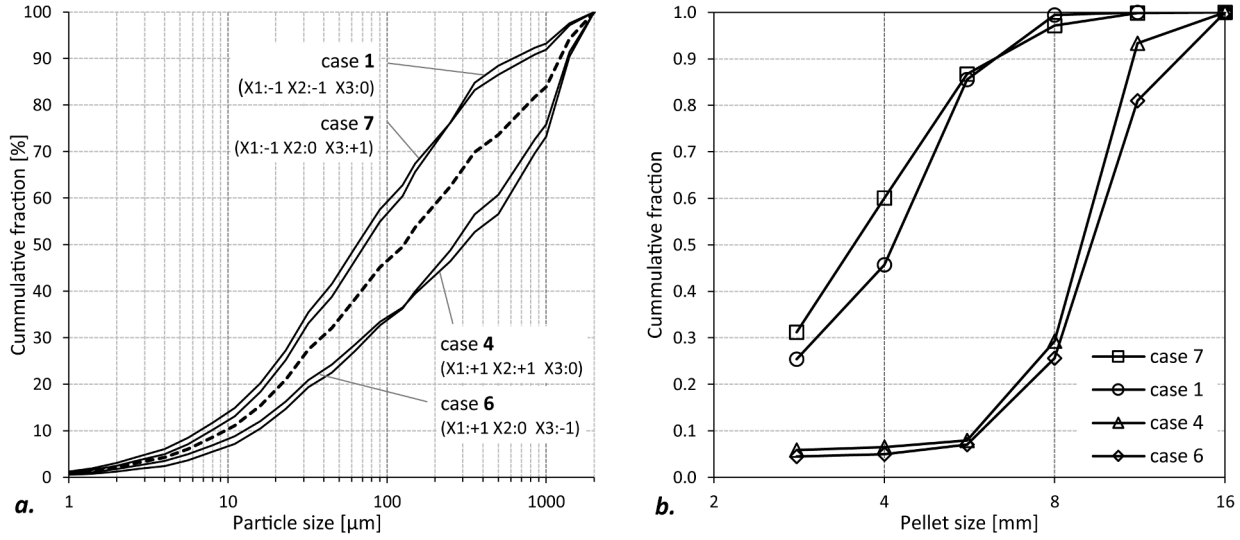

Fig. 5. *a*: Estimated particle size distribution of raw material mixes for cases 1, 4, 6 and 7, and for central cases (dashed line). *b*: sieving analysis of pellets obtained.

Table 5
ANOVA: particle densities.

	Particle density, SSD						Particle density, oven-dry					
Source	*Coefficient*[g/cm^3·10^3]	*SS*	*df*	*MS*	*F*	*p*	*Coefficient*[g/cm^3·10^3]	*SS*	*df*	*MS*	*F*	*p*
Model		0.063	10	0.006	5.515	0.024		0.221	10	0.022	4.96	0.031
intercept	1.668	4.174	1	4.174	3666.370	< 0.001	1.480	3.285	1	3.285	737.098	< 0.001
block	0.016	0.004	1	0.004	3.919	0.095	**0.053**	0.046	1	0.046	10.429	**0.018**
Bc/B	0.004	0.000	1	0.000	0.086	0.779	**-0.092**	0.068	1	0.068	15.358	**0.008**
B/S	**-0.068**	0.037	1	0.037	32.253	**0.001**	**-0.071**	0.040	1	0.040	8.953	**0.024**
c/C	0.003	0.000	1	0.000	0.044	0.841	0.053	0.022	1	0.022	5.018	0.066
Bc/B · B/S	-0.002	0.000	1	0.000	0.011	0.919	-0.022	0.002	1	0.002	0.427	0.538
Bc/B · c/C	-0.013	0.001	1	0.001	0.594	0.470	0.034	0.005	1	0.005	1.053	0.344
B/S · c/C	0.000	0.000	1	0.000	0.000	0.992	0.074	0.018	1	0.018	3.927	0.095
$(Bc/B)^2$	**-0.060**	0.015	1	0.015	13.220	**0.011**	-0.063	0.017	1	0.017	3.753	0.101
$(B/S)^2$	0.024	0.002	1	0.002	2.039	0.203	0.013	0.001	1	0.001	0.160	0.703
$(c/C)^2$	-0.014	0.001	1	0.001	0.768	0.414	-0.028	0.003	1	0.003	0.734	0.424
Residuals		0.007	6	0.001				0.027	6	0.004		
Corr. Total		0.070	16					0.248	16			

Table 6
ANOVA: water absorption capacity and drying shrinkage.

	Water absorption capacity (oven-dry to SSD)						Volumetric drying shrinkage (SDD to oven-dry)					
Source	*Coefficient*[% dry m.]	*SS*	*df*	*MS*	*F*	*p*	*Coefficient*[% SSD v.]	*SS*	*df*	*MS*	*F*	*p*
Model		0.057	10	0.006	5.942	0.020		0.058	10	0.006	1.700	0.266
intercept	43.60	0.285	1	0.285	295.269	< 0.001	21.40	0.069	1	0.069	20.090	0.004
block	-0.80	0.001	1	0.001	1.232	0.310	1.30	0.003	1	0.003	0.881	0.384
Bc/B	**-3.60**	0.010	1	0.010	10.748	**0.017**	**-6.80**	0.037	1	0.037	10.708	**0.017**
B/S	**7.30**	0.043	1	0.043	44.652	**0.001**	3.20	0.008	1	0.008	2.435	0.170
c/C	-0.50	0.000	1	0.000	0.197	0.673	2.20	0.004	1	0.004	1.095	0.336
Bc/B · B/S	-0.20	0.000	1	0.000	0.019	0.895	-1.40	0.001	1	0.001	0.218	0.657
Bc/B · c/C	-1.40	0.001	1	0.001	0.872	0.386	1.80	0.001	1	0.001	0.359	0.571
B/S · c/C	0.90	0.000	1	0.000	0.262	0.627	4.00	0.005	1	0.005	1.486	0.269
$(Bc/B)^2$	0.80	0.000	1	0.000	0.245	0.638	-0.40	0.000	1	0.000	0.022	0.888
$(B/S)^2$	0.20	0.000	1	0.000	0.022	0.886	-0.80	0.000	1	0.000	0.087	0.778
$(c/C)^2$	0.20	0.000	1	0.000	0.013	0.911	-0.10	0.000	1	0.000	0.002	0.968
Residuals		0.006	6	0.001				0.020	6	0.003		
Corr. Total		0.063	16					0.079	16			

Table 7
ANOVA: particle crushing strength at 7 and 70 days.

	7-day strength						70-day strength					
Source	*Coefficient* [MPa]	*SS*	*df*	*MS*	*F*	*p*	*Coefficient* [MPa]	*SS*	*df*	*MS*	*F*	*p*
Model		3.714	10	0.3714	10.658	0.005		3.864	10	0.3864	1.372	0.362
intercept	0.077	0.009	1	0.009	0.257	0.630	0.944	1.337	1	1.337	4.748	0.072
block	0.025	0.011	1	0.011	0.305	0.600	-0.049	0.040	1	0.040	0.144	0.718
Bc/B	**0.443**	1.573	1	1.573	45.137	**0.001**	**0.502**	2.014	1	2.014	7.152	**0.037**
B/S	**-0.242**	0.468	1	0.468	13.433	**0.011**	-0.303	0.732	1	0.732	2.599	0.158
c/C	**0.284**	0.645	1	0.645	18.519	**0.005**	0.109	0.095	1	0.095	0.338	0.582
Bc/B · B/S	-0.116	0.051	1	0.051	1.462	0.272	-0.082	0.025	1	0.025	0.090	0.774
Bc/B · c/C	0.196	0.153	1	0.153	4.388	0.081	-0.146	0.085	1	0.085	0.303	0.602
B/S · c/C	**-0.308**	0.306	1	0.306	8.787	**0.025**	-0.389	0.488	1	0.488	1.732	0.236
$(Bc/B)^2$	0.204	0.174	1	0.174	5.001	0.067	-0.166	0.115	1	0.115	0.410	0.546
$(B/S)^2$	0.111	0.052	1	0.052	1.481	0.269	0.070	0.021	1	0.021	0.074	0.795
$(c/C)^2$	0.160	0.107	1	0.107	3.067	0.130	-0.268	0.300	1	0.300	1.064	0.342
Residuals		0.209	6	0.035				1.690	6	0.282		
C. Total		3.923	16					5.554	16			

(opposite sign interaction, reducing the first order effect). In addition to these statistically significant effects, coarse sawdust ratio, *Bc/B*, appeared to have a second order effect on 7-day strength, judging from the magnitude of its coefficient (Fig. 6).

The ANOVA of the 70-day strength response model (also in Table 7) shows that the factors can only partially explain the observed variations (model $p = 0.362$). In contrast with the 7-day strength model, the ANOVA shows that only the coarse sawdust ratio, *Bc/B*, had a significant effect on the response. According to the corresponding model coefficient, 70-day particle crushing strength of the pellets increases when the coarse sawdust ratio is increased. Although not reaching the required significance level, the sawdust content, *B/S*, appears to also affect 70-day strength (second smallest *p*-value). According to the corresponding coefficient, 70-day particle crushing strength of the pellets decreases when the sawdust content increases. These two effects are consistent with those observed on 7-day strength.

In both, 7-day and 70-day, response models, the coarse sawdust ratio, *Bc/B*, displays the largest effect. The cause of the effect cannot be determined solely from the results of the explorative experiment. The positive effect of higher coarse sawdust ratios could, for instance, be the

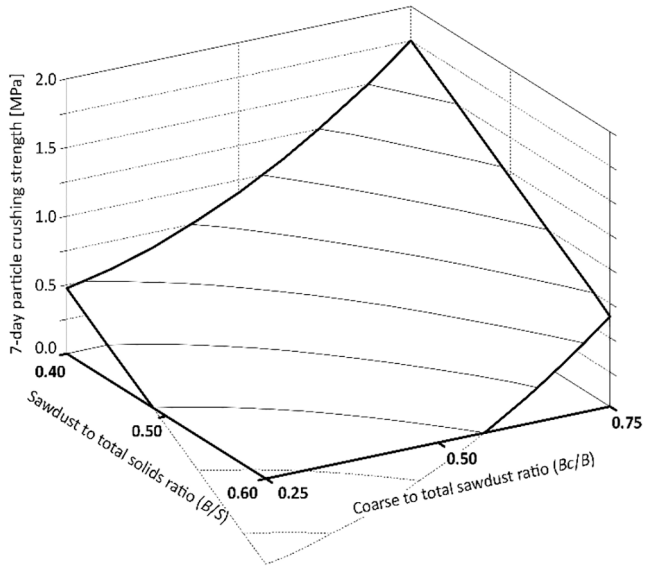

Fig. 6. Response surface of particle crushing strength at 7 days, considering all factors and interactions with p-values < 0.10. The plotted surface corresponds to predicted response when all cement dose is intermixed in the raw materials mixture ($c/C = 1$).

result of avoiding negative impacts from the wood dust – which could arise from chemical additives likely present in it (e.g. glues, impermeabilization compounds, coloring agents). However, the fact that pellet stickiness also increased at higher coarse sawdust ratios might indicate that chemical or physical reactions occur at the interfaces between coarse sawdust particles, or between them and other solids in the raw mix (e.g. ashes). The same reactions taking place at the surface of pellets – causing strong particle bonding during storage – could also take place inside them, contributing to particle crushing strength. Experiments required to test these hypotheses could not be carried out within the scope of the reported research. Nevertheless, the observed factor-response relationship was validated beyond the range explored in the main experiment in the third experimental campaign.

Large variations in strength gain over time were observed, including between central cases. Variations between central cases indicate that external factors were affecting the response. Accordingly, in the ANOVA of the strength-gain response model none of the studied factors, nor the model itself, reached the required significance level.

In some of the experiment cases, a large variability was observed between single-pellet strength results. As seen in Table 2, the coefficient of variation (CV) ranged from 13% to 146% the average value in the case of 7-day strength measurements, and from 11% to 305% the average value for 70-day measurements. Regression was used to model the factor-response relationship of the 70-day particle crushing strength CV in an attempt to identify the major sources of variability. Although the ANOVA of the model (Table 8) shows it can only partially explain the observed variation (model $p = 0.196$), two factors appeared to have a significant effect on the CV. According to the model, the CV of the 70-day particle crushing strength of the pellets decreases when the fraction of the cement dose incorporated in the raw materials mix, c/C, is increased. In other words, intermixing the cement dose with the rest of the raw materials results in less variation in the individual particle strength of the pellets, compared to using it as a coating. The effect is evident in Fig. 7, where it can be seen that it is also present on the CV of 7-day strength. Incorporating the cement with the rest of the raw materials resulted in a more homogeneous product thanks to the pre-mixing that takes place prior to the pelletization process. Conversely, achieving a homogeneous coating by dispersing a relatively small dose of cement over the rolling pellets is difficult. A much larger cement dose would be

Table 8
ANOVA: within-case CV of 70-day strength.

Source	*Coefficient* [C.V.]	*SS*	*df*	*MS*	*F*	*p*
Model		2.040	10	0.204	2.050	0.196
intercept	0.836	1.048	1	1.048	10.527	0.018
block	-0.024	0.009	1	0.009	0.093	0.770
Bc/B	-0.086	0.060	1	0.060	0.598	0.469
B/S	-0.035	0.010	1	0.010	0.098	0.764
c/C	**-0.356**	1.015	1	1.015	10.199	**0.019**
Bc/B · B/S	0.066	0.016	1	0.016	0.164	0.700
Bc/B · c/C	0.055	0.012	1	0.012	0.122	0.739
B/S · c/C	-0.101	0.033	1	0.033	0.331	0.586
$(Bc/B)^2$	**-0.461**	0.890	1	0.890	8.940	**0.024**
$(B/S)^2$	-0.009	0.000	1	0.000	0.003	0.958
$(c/C)^2$	0.004	0.300	1	0.300	0.001	0.980
Residuals		0.597	6	0.100		
C. Total		2.638	16			

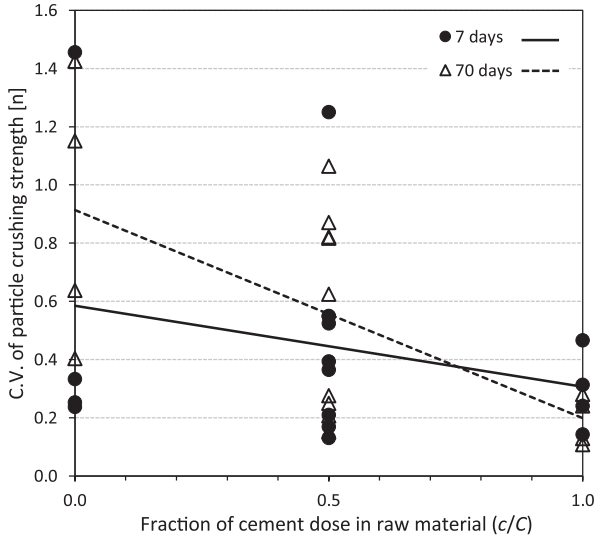

Fig. 7. Within-case CV of particle crushing strength tests at 7 and 70 days versus fraction of cement dose included in the raw materials mix (c/C).

needed to achieve higher homogeneity. A coating can perform relevant functions in specific applications, such as improving encapsulation of potentially harmful compounds in the raw materials [21] or preventing leakage of phase change materials in pellets intended to modify the thermal properties of concrete [25,37]. However, considering the negative impact of Portland cement on the environmental footprint of the pellets, the findings reported here show that its use as a coating cannot be justified solely from a mechanical performance point of view.

The coarse sawdust ratio, Bc/B, also appeared to have a significant effect on CV, although of second order. According to the corresponding model coefficient, the CV of 70-day strength tests is maximum when coarse and fine sawdust are mixed in equal parts, but decreases away from that value. A possible explanation for this effect lies in the difficulty of obtaining a homogeneous mixture of different sawdust sizes: mixture homogeneity is expected to increase as the ratio of coarse to fine particles approaches either 1 or 0. The effects of these two factors on the within-case CV of particle crushing strength align with their direct effects on the response: For a given cement dose, incorporating all cement in the raw materials mix maximizes strength and reduces strength variability among individual pellets. Likewise, for a given sawdust content, using only coarse sawdust maximizes strength and reduces strength variability among individual pellets.

Strength results were checked for correlation with effective cement content – as the latter varied among cases as a result of variations in pelletization output volume. As seen in Fig. 8, cement dose cannot

explain the observed variation in particle crushing strength among cases, neither at 7 nor at 70 days after production. Neither had the cement dose an evident influence on the strength gain over time (vertical lines in the Figure). This implies that there is an optimal set of raw material ratios that maximizes the particle crushing strength of the pellets at any given cement dose, or, in other words, minimizes the amount of cement required to achieve a given target strength.

4.5. Follow-up experiments (validation)

Follow up experiments were carried out to test the factor-response relationships previously identified, using them to optimize pellet properties. As lightweight aggregates, desirable pellet properties are high strength, low density and low hygroscopic expansion/shrinkage (which correlates with lower water absorption capacity). However, the response models show these properties to be affected differently by the different factors. In order to identify beneficial directions of change in the factor levels, an overall quality index was defined as a function of the three properties as shown in eq. (4):

$$Quality = R_{7-day}/(D_{SSD} \cdot S_{SSD>dry}) \quad (4)$$

where, $R_{7\text{-}day}$ is the particle crushing strength at 7 days, D_{SSD} is the particle density in SSD condition and $S_{SSD>dry}$ is the volumetric shrinkage from SSD to dry condition of the pellets. As defined, higher index values indicate better quality pellets (i.e. higher strength, lower density, lower shrinkage/expansion and lower water absorption). Across the cases in the factorial experiment, the unitless index ranged from 0.04 to 4.58. As in the case of individual properties, the factor-quality relationship was modeled using linear regression. Owing to the large variation in strength among cases – compared to the variation in density and shrinkage –, the quality model highly resembles the strength response model. Results from the ANOVA of the model (Table 9) show that all main factors had significant effects on the quality. According to the model coefficients, quality increases when the coarse sawdust ratio, Bc/B, is increased and when the fraction of the cement dose incorporated in the raw materials mix, c/C, is increased, and decreases when the total sawdust content, B/S, is increased. The model also shows that the effect of the fraction of cement incorporated in the raw material mix depends on the total sawdust content ($B/S \cdot c/C$ interaction effect), the effect being much stronger at lower sawdust contents but slightly reversing at high sawdust contents.

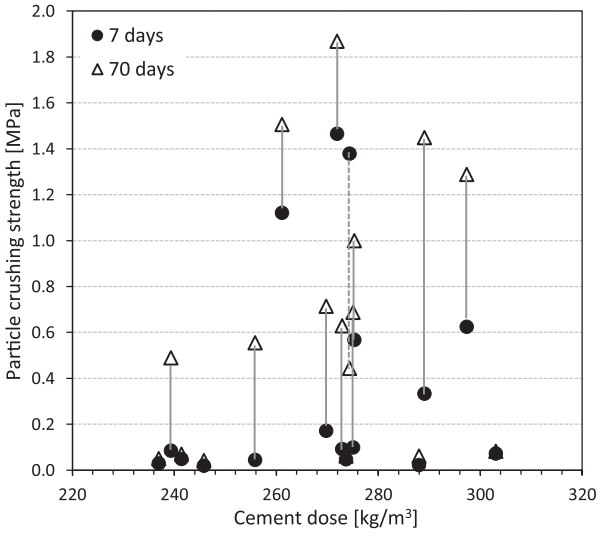

Fig. 8. Particle crushing strength at 7 and 70 days versus actual cement dose (estimated per m^3 of solid volume from process output and density measurements). Vertical lines represent strength gain between the two testing dates.

Table 9
ANOVA: quality index.

Source	*Coefficient* [*]	*SS*	*df*	*MS*	*F*	*p*
Model		38.877	10	3.888	6.249	**0.018**
intercept	0.642	0.426	1	0.426	0.945	0.440
block	−0.054	0.022	1	0.022	0.076	0.857
Bc/B	**1.618**	19.854	1	19.854	32.037	**0.001**
B/S	**−0.731**	4.644	1	4.644	6.537	**0.034**
c/C	**0.675**	4.076	1	4.076	5.569	**0.043**
$Bc/B \cdot B/S$	−0.388	0.591	1	0.591	0.868	0.367
$Bc/B \cdot c/C$	0.267	0.347	1	0.347	0.436	0.483
$B/S \cdot c/C$	**−1.065**	3.910	1	3.910	5.610	**0.046**
$(Bc/B)^2$	0.833	2.677	1	2.677	4.444	0.083
$(B/S)^2$	0.551	1.468	1	1.468	1.948	0.175
$(c/C)^2$	0.148	0.195	1	0.195	0.141	0.596
Residuals		3.733	6	0.622		
C. Total		42.610	16			

* arbitrary units (see eq. (4))

Since all significant effects are linear, all three factors would have to be brought to their limiting ratios (0 or 1) in order to maximize pellet quality. However, unlike using only coarse sawdust ($Bc/B = 1$) or incorporating all the cement dose in the raw materials mix ($c/C = 1$), not using any sawdust ($B/S = 0$) would completely change the nature of the material and negate the original research purpose. Accordingly, the follow-up cases where formulated to test the effect of sawdust content on pellet properties when only coarse sawdust is used ($Bc/B = 1$) and all the cement dose is intermixed with the rest of the raw materials ($c/C = 1$).

4.6. Additional, validation cases

The factor levels and the observed responses from the additional cases are shown in Table 10. The results confirmed the predictions of the response models derived from the factorial exploration. In all but one of the follow-up cases, the particle crushing strength at 7-days was higher than the maximum observed in the factorial exploration, confirming the estimated effect of the coarse sawdust ratio (Fig. 9a). Particle densities followed the same trend observed in the factorial exploration, increasing as sawdust content decreases. As seen in Fig. 9b, cases at similar sawdust contents exhibited similar densities in both experiments. Drying shrinkages were comparable to the lowest observed in the factorial experiment, confirming the effect of the coarse sawdust ratio (Fig. 9c). As a consequence of these results, all additional cases achieved quality indexes exceeding the maximum recorded in the factorial exploration.

In accordance with the strength response model derived from the factorial experiment, in the follow-up cases, particle crushing strength was observed to decrease as sawdust content increases. However, as seen in Fig. 10, the negative effect of higher sawdust contents was less pronounced when all sawdust was coarse compared to when it was mixed with finer sawdust (lower coarse sawdust ratios). Although no significant interaction between sawdust content and coarse sawdust ratio was identified in the factorial experiment, the graphical comparison provides clear evidence of dependency. These results point out the need to perform preliminary trials when alternative sawdust sources are available, and serve as a reminder that the validity of the estimated effects is limited to the specific materials studied.

In agreement with findings from the factorial experiment, in the follow-up cases correlation was observed between sawdust content and water uptake during pelletization, and therefore between water uptake and pellet strength. The replication of case 18 (18b in Table 10) was used as an opportunity to distinguish the effects of sawdust content and water uptake on strength. In line with observations found in the literature [38], different water uptakes were achieved by allowing the material in case 18b a longer time to agglomerate before adding additional water. At identical sawdust contents, the case with the lowest water uptake exhibited the highest strength. This observation indicates that higher

Table 10
Results from additional experimental cases in execution order.

		Factors (empirical levels)			Production				Pellet properties								
					Water uptake	Output mass	Output volume	Cement dose	-	Fineness	Stick.	Density (mass/volume) ssd/ssd	dry/ssd	dry/dry	W. abs. capacity	Drying shrinkage	Strength 7 days	Quality Index
Block	Case	*Bc/B*	*B/S*	*c/C*	[L/Kg]	[kg]	[cm^3]	[kg/m^3]	-	[*]	[arb.]	[g/cm^3]	[g/cm^3]	[g/cm^3]	[% dry m.]	[% sat.v.]	[MPa]	[–]
5	18	1.0	0.3	1.0	0.23	8.50	4588	262		0.31	1.50	1.868	1.509	1.781	23.8	15.2	1.60	5.62
	20	1.0	0.5	1.0	0.35	6.70	3917	306		0.25	1.50	1.678	1.268	1.472	32.3	13.9	1.59	6.85
	19	1.0	0.4	1.0	0.31	7.73	4526	265		0.30	2.00	1.713	1.303	1.564	31.5	16.7	1.31	4.60
	18b	1.0	0.3	1.0	0.21	8.38	4225	284		0.33	1.00	1.983	1.639	1.854	21.0	11.6	1.75	7.60

strengths could be obtained in this way, albeit at the expense of higher particle densities.

4.7. Summary of findings

A qualitative summary of the significant effects observed within the experimental region explored is presented in Table 11. It shows that the sawdust to total solids ratio (*B/S*) and the coarse to total sawdust ratio (*Bc/B*) exhibited opposing effects on several responses. Thus, the negative impacts of higher sawdust contents (i.e. higher water demand, higher water absorption capacity, higher hygroscopic shrinkage and lower crushing strength) are reduced when coarser sawdust is used.

In addition, the embodied energy (EE) and global warming potential (GWP) linked to the production of the pellets were estimated for the validation cases, using available life cycle inventory data [39] and considering the contribution of raw materials, transport, and fabrication. The uncompacted, bulk volume of the pellets was chosen as the unit of analysis, being a good estimator for the pellet quantity required to make a cubic meter of lightweight concrete without adding other aggregate. As such, the estimated values represent the contribution of the pellets to EE and GWP of the concrete. The average estimated EE of the pellets was to 213 kWh/m^3, of which 192 kWh (i.e. 90%) were due to Portland cement used as binder. The average estimated GWP of the pellets was 134 kgCO_2eq/m^3, of which 128 kgCO_2eq (i.e. 95%) were due to the cement.

5. Conclusions

The reported research explored and verified the feasibility of producing lightweight aggregates by cold-bonding of biomass wastes and demonstrated how their properties can be controlled by adjustments to the proportions of the raw materials. Aggregates were produced by pelletizing mixtures of coarse sawdust from spruce, fine sawdust from MDF processing, wood ashes from thermal energy production, and Portland cement. Results showed that aggregates with particle densities below 1.850 g/cm^3 (oven dry) and particle crushing strengths above 1.5 MPa can be obtained from these mixtures with cement doses as low as 260 kg/m^3 of solids.

Raw material mixtures were described using three ratios: 1) the sawdust to total solids ratio (*B/S*), explored in the range 0.40 to 0.60 by volume, 2) the coarse sawdust to total sawdust ratio (*Bc/B*), explored in the range 0.25 to 0.75 by volume, and 3) the ratio of cement intermixed in the raw materials – as opposed to added as a coating to the already formed pellets – versus total cement dose (*c/C*), explored between 0.0 and 1.0, for a fixed target cement dose of 240 kg/m^3 of pellets (solids volume). The effects of adjustments to these ratios were studied using response surface methodology. All raw material ratios were observed to distinctly affect several aggregate properties simultaneously. Although this means that individual properties cannot be controlled independently, an advantageous combination of properties can be achieved by balancing the opposing effects that different ratios have on specific properties. Lightweight aggregates are obtained by adding sawdust to the raw material mixture, but increasing sawdust contents significantly increases the water absorption capacity and drying shrinkage of the aggregates, and reduces their short- and long-term strength. At all explored sawdust contents, increasing the coarse to total sawdust ratio reduced water absorption and drying shrinkage of the aggregates, and increased their short- and long-term strength, partially compensating the negative effects of higher sawdust contents while further decreasing particle density. Most likely, microstructural features of wood, present in the coarse sawdust particles, provide an internal constraint to water absorption and hygroscopic dimensional changes and contribute to strength, but are lost in the finer sawdust. Increasing the coarse to total sawdust ratio also reduced the water demand during the pelletization process, but increased the average size of the pellets (i.e. reduced the fineness) and lead to increased superficial bonding of freshly made

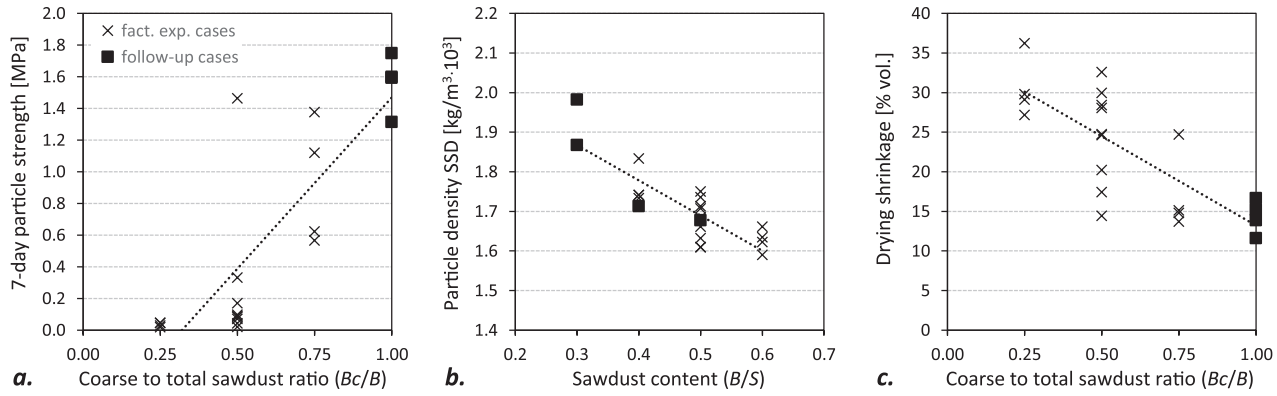

Fig. 9. Results from follow-up cases compared to results from factorial experiment cases: *a*. 7-day particle crushing strength, *b*. particle density in SSD condition, and *c*. volumetric drying shrinkage. In all graphs, factorial cases and follow-up cases are marked by crosses and filled squares, respectively (see graph *a*).

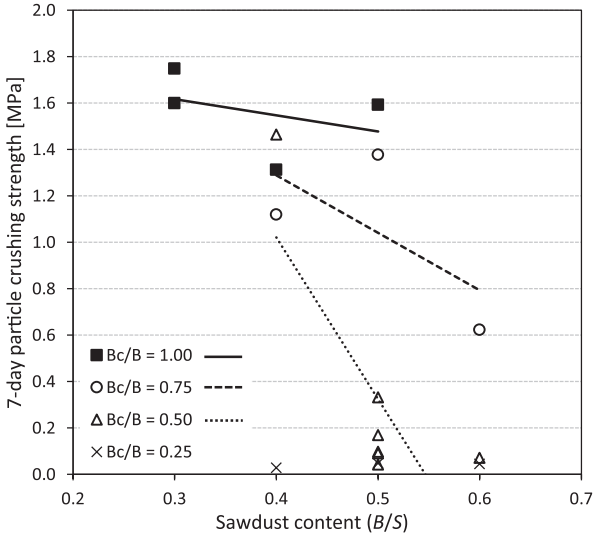

Fig. 10. 7-day particle crushing strength versus sawdust content (*B/S*) at different levels of coarse sawdust ratios (*Bc/B*). The graph displays only those cases where at least 50% of the cement dose was intermixed with the raw materials.

Table 11
Effects of raw material ratios change (increase) on the properties of obtained aggregates.

Properties	Raw material ratios		
	B/S 0.4–0.6	*Bc/B* 0.25–0.75	*c/C* 0–1
Water demand (for pelletization)	+	–	0
Stickiness (during storage)	0	+	0
Fineness (particle size distribution)	0	–	(+)
Particle density: saturated surface dry	–	–[2]	0
Particle density: oven dry	–	–	(+)
Water absorption capacity	+	–	0
Drying shrinkage	(+)	–	0
Particle crushing strength: 7 days	–	+ (+[2])	+ –[i]
Particle crushing strength: 70 days	(–)	+	0
CV of 70-day strength	0	–[2]	–

Notes:
+ Positive effect
– Negative effect
(…) Large effect coefficient but not reaching significance level
[2] Second order effect
[i] Interaction with another factor

pellets during storage (i.e. increased stickiness). Very large pellets were formed upon incorporation of initial water to the pelletizer. Destroying these initial pellets allowed better distribution of moisture in the raw material mix which, in turn, resulted in smaller pellets reforming.

Intermixing the cement dose with the raw materials also contributed to reduce pellet size. In addition, increasing the fraction of the cement dose intermixed with the raw materials increased short-term particle crushing strength and, most notably, reduced strength variability between particles. Consequently, – and as demonstrated in the validation experiments –, for the specific set of raw materials used in the reported study, at cement doses between 240 and 300 kg/m^3 and sawdust contents between 30% and 60% by volume of raw materials, lighter, consistently stronger, less water demanding and more dimensionally stable lightweight aggregates are achieved by using coarse sawdust only and by intermixing all of the cement dose in the raw materials mixture.

Several aspects of LWA performance need to be investigated directly in lightweight concrete mixes. This includes not only their impact on mechanical performance but also the impact of water absorption dynamics and hygroscopic shrinkage/expansion of the aggregate on the fresh and hardened properties of concrete. The impact of the aggregates on the fire and heat resistance of the concrete and on its overall thermal performance also needs to be explored. In addition to testing these effects, further research will focus on exploring additional raw materials that can undergo cementitious reactions with compounds present in the wood ashes, enabling replacement of Portland cement. While production of LWA by cold-bonding can be a valuable use for locally available biomass waste, using Portland cement as binder severely limits the environmental benefits by significantly increasing its embodied energy and global warming potential.

CRediT authorship contribution statement

Ricardo Serpell: Conceptualization, Methodology, Validation, Formal analysis, Investigation, Writing – original draft, Writing – review & editing, Visualization, Project administration, Funding acquisition. **Daia Zwicky:** Conceptualization, Resources, Writing – review & editing, Supervision, Funding acquisition.

Declaration of Competing Interest

The authors declare that they have no known competing financial interests or personal relationships that could have appeared to influence the work reported in this paper.

Data availability

Data will be made available on request.

Acknowledgments

The reported research was made possible by funding from the Smart Living Lab (SLL) research and development center in Fribourg, Switzerland. We also acknowledge the support of the Haute école d'ingénierie et d'architecture de Fribourg. We thank in particular Mr. Niccolò Macchi, scientific collaborator at iTEC, for his contribution to the project, and the civil engineering lab technicians: Yanis Schaller, Jonathan Moix, Dominique Delaquis and Benjamin Frei, for their help. Finally, we are grateful to the companies that sourced biomass wastes for the development of the empirical exploration program: Yerly Bois SA (coarse sawdust) and SAK St. Gallisch-Appenzellische Kraftwerke AG (wood ashes).

References

[1] Lignum, Bulletin bois (Holzbulletin), (n.d.). https://www.lignum.ch/fr/prestations/produits/bulletin_bois/ (accessed March 17, 2022).
[2] L. Tschümperlin, L. Ramseier, R. Frischknecht, treeze Ltd., Ökobilanz ausgewählter Betonsorten: Fachstelle nachhaltiges Bauen, Fachstelle Ingenieurwesen, Zürich, 2020.
[3] J. Anderson, A. Moncaster, Embodied carbon of concrete in buildings, Part 1: analysis of published EPD, Build, Cities. 1 (2020) 198–217, https://doi.org/10.5334/bc.59.
[4] M. Li, M. Khelifa, M. El Ganaoui, Mechanical characterization of concrete containing wood shavings as aggregates, Int. J. Sustain. Built Environ. 6 (2017) 587–596, https://doi.org/10.1016/j.ijsbe.2017.12.005.
[5] Y.X.X. Chen, F. Wu, Q. Yu, H.J.H.J.H. Brouwers, Bio-based ultra-lightweight concrete applying miscanthus fibers: acoustic absorption and thermal insulation, Cem. Concr. Compos. 114 (2020), 103829, https://doi.org/10.1016/j.cemconcomp.2020.103829.
[6] W. Ahmed, R.A. Khushnood, S.A. Memon, S. Ahmad, W.L. Baloch, M. Usman, Effective use of sawdust for the production of eco-friendly and thermal-energy efficient normal weight and lightweight concretes with tailored fracture properties, J. Clean. Prod. 184 (2018) 1016–1027, https://doi.org/10.1016/j.jclepro.2018.03.009.
[7] D. Zwicky, Mechanical properties of organic-based lightweight concretes and their impact on economic and ecological performances, Constr. Build. Mater. 245 (2020) 118413.
[8] D. Zwicky, N. Macchi, Wood-Based Concrete for Composite Building Construction with Timber. Concr. Innov. Conf. CIC2014, Oslo, Norway, 2014.
[9] F.C. Jorge, C. Pereira, J.M.F. Ferreira, Wood-cement composites: a reviewHolz-Zement-Werkstoffe: Ein berblick, Holz Roh Werkst. 62 (5) (2004) 370–377.
[10] D. Zwicky, Combustibility of wood-cement compounds, in: 10th Conf. Adv. Build. Ski., Bern, 2015, pp. 164–172.
[11] F. Berger, F. Gauvin, H.J.H. Brouwers, The recycling potential of wood waste into wood-wool/cement composite, Constr. Build. Mater. 260 (2020), 119786, https://doi.org/10.1016/J.CONBUILDMAT.2020.119786.
[12] B. Na, Z. Wang, H. Wang, X. Lu, Wood-cement compatibility review, Wood Res. 59 (2014) 813–826.
[13] F. Tajra, M.A. Elrahman, D. Stephan, The production and properties of cold-bonded aggregate and its applications in concrete: A review, Elsevier Ltd 225 (2019) 29–43, https://doi.org/10.1016/j.conbuildmat.2019.07.219.
[14] S.N. Chinnu, S.N. Minnu, A. Bahurudeen, R. Senthilkumar, Recycling of industrial and agricultural wastes as alternative coarse aggregates: A step towards cleaner production of concrete, Constr. Build. Mater. 287 (2021), 123056, https://doi.org/10.1016/j.conbuildmat.2021.123056.
[15] C. Narattha, A. Chaipanich, Phase characterizations, physical properties and strength of environment-friendly cold-bonded fly ash lightweight aggregates, J. Clean. Prod. 171 (2018) 1094–1100, https://doi.org/10.1016/j.jclepro.2017.09.259.
[16] N.U. Kockal, T. Ozturan, Characteristics of lightweight fly ash aggregates produced with different binders and heat treatments, Cem. Concr. Compos. 33 (2011) 61–67, https://doi.org/10.1016/j.cemconcomp.2010.09.007.
[17] E. Güneyisi, M. Gesoğlu, Ö. Pürsünlü, K. Mermerdaş, Durability aspect of concretes composed of cold bonded and sintered fly ash lightweight aggregates, Compos. Part B Eng. 53 (2013) 258–266, https://doi.org/10.1016/j.compositesb.2013.04.070.
[18] E. Güneyisi, M. Gesoğlu, I. Altan, H.Ö. Öz, Utilization of cold bonded fly ash lightweight fine aggregates as a partial substitution of natural fine aggregate in self-compacting mortars, Constr. Build. Mater. 74 (2015) 9–16, https://doi.org/10.1016/j.conbuildmat.2014.10.021.
[19] L.A.T. Bui, C.L. Hwang, C.T. Chen, K.L. Lin, M.Y. Hsieh, Manufacture and performance of cold bonded lightweight aggregate using alkaline activators for high performance concrete, Constr. Build. Mater. 35 (2012) 1056–1062, https://doi.org/10.1016/j.conbuildmat.2012.04.032.
[20] S. Geetha, K. Ramamurthy, Environmental friendly technology of cold-bonded bottom ash aggregate manufacture through chemical activation, J. Clean. Prod. 18 (2010) 1563–1569, https://doi.org/10.1016/j.jclepro.2010.06.006.
[21] F. Colangelo, F. Messina, R. Cioffi, Recycling of MSWI fly ash by means of cementitious double step cold bonding pelletization: technological assessment for the production of lightweight artificial aggregates, J. Hazard. Mater. 299 (2015) 181–191, https://doi.org/10.1016/j.jhazmat.2015.06.018.
[22] F. Colangelo, I. Farina, R. Penna, L. Feo, F. Fraternali, R. Cioffi, Use of MSWI fly ash for the production of lightweight artificial aggregate by means of innovative cold bonding pelletization technique. Chemical and morphological characterization, Chem. Eng. Trans. 60 (2017) 121–126, https://doi.org/10.3303/CET1760021.
[23] C.L. Hwang, V.A. Tran, A study of the properties of foamed lightweight aggregate for self-consolidating concrete, Constr. Build. Mater. 87 (2015) 78–85, https://doi.org/10.1016/J.CONBUILDMAT.2015.03.108.
[24] F. Tajra, M.A. Elrahman, S.-Y. Chung, D. Stephan, Performance assessment of core-shell structured lightweight aggregate produced by cold bonding pelletization process, Constr. Build. Mater. 179 (2018) 220–231, https://doi.org/10.1016/j.conbuildmat.2018.05.237.
[25] S. Drissi, T.-C.-C. Ling, K.H. Mo, Development of leak-free phase change material aggregates, Constr. Build. Mater. 230 (2020), 117029, https://doi.org/10.1016/j.conbuildmat.2019.117029.
[26] F.C. Bergeron, Energy and climate impact assessment of waste wood recovery in Switzerland, Biomass Bioenergy. 94 (2016) 245–257, https://doi.org/10.1016/J.BIOMBIOE.2016.09.009.
[27] A. Sarabèr, R. Overhof, T. Green, J. Pels, Artificial lightweight aggregates as utilization for future ashes - A case study, Waste Manag. 32 (2012) 144–152, https://doi.org/10.1016/j.wasman.2011.08.017.
[28] N.M. Sigvardsen, M.R. Geiker, L.M. Ottosen, Reaction mechanisms of wood ash for use as a partial cement replacement, Constr. Build. Mater. 286 (2021), 122889, https://doi.org/10.1016/j.conbuildmat.2021.122889.
[29] V. Gryc, P. Horáček, J. Šlezingerová, H. Vavrčík, Basic Density of Spruce Wood, Wood with Bark, and Bark of Branches in Locations in the Czech Republic, Wood Res. 56 (2011) 23–32.
[30] E. Meier, Norway Spruce | Lumber Identification (Softwood), Wood Database. (n.d.). https://www.wood-database.com/norway-spruce/ (accessed May 28, 2021).
[31] CEN, EN 1097-6:2013 (E) Tests for mechanical and physical properties of aggregates. Part 6: Determination of particle density and water absorption, (2013) 49.
[32] J. Srb, Z. Ruzickova, Pelletization of fines, Elsevier Science Ltd., Amsterdam, NL, 1988.
[33] G.E.P. Box, D.W. Behnken, Some new three level designs for the study of quantitative variables, Technometrics. 2 (1960) 455–475, https://doi.org/10.1080/00401706.1960.10489912.
[34] P. Vasanthi, S. Senthil Selvan, P. Murthi, I. Rajasri Reddy, K. Poongodi, Impact of partial replacement of cement by coconut shell ash and coarse aggregate by coconut shell on mechanical properties of concrete, IOP Conf. Ser. Mater. Sci. Eng. 981 (3) (2020) 032080.
[35] A. Sujatha, S.D. Balakrishnan, Properties of Coconut Shell Aggregate Concrete: A Review, in: R.M. Singh, K.P. Sudheer, B. Kurian (Eds.), Adv. Civ. Eng. Lect. Notes Civ. Eng., Springer, Singapore, 2021, pp. 759–769, https://doi.org/10.1007/978-981-15-5644-9_60.
[36] M. Bernhardt, H. Tellesbø, H. Justnes, K. Wiik, Mechanical properties of lightweight aggregates, J. Eur. Ceram. Soc. 33 (2013) 2731–2743, https://doi.org/10.1016/j.jeurceramsoc.2013.05.013.
[37] E.Y. Tuncel, B.Y. Pekmezci, A sustainable cold bonded lightweight PCM aggregate production: Its effects on concrete properties, Constr. Build. Mater. 181 (2018) 199–216, https://doi.org/10.1016/j.conbuildmat.2018.05.269.
[38] K.I. Harikrishnan, K. Ramamurthy, Influence of pelletization process on the properties of fly ash aggregates, Waste Manag. 26 (2006) 846–852, https://doi.org/10.1016/J.WASMAN.2005.10.012.
[39] KBOB Switzerland, Ökobilanzdaten im Baubereich 2009/1:2016, Bern, Switzerland, 2016.